Proposing a High-Precision Petroleum Pipeline Monitoring System for Identifying the Type and Amount of Oil Products Using Extraction of Frequency Characteristics and a MLP Neural Network

Abdulilah Mohammad Mayet [1] , **Karina Shamilyevna Nurgalieva** [2] , **Ali Awadh Al-Qahtani** [1],
Igor M. Narozhnyy [3], **Hala H. Alhashim** [4], **Ehsan Nazemi** [5],* and **Ilya M. Indrupskiy** [6]

1   Electrical Engineering Department, King Khalid University, Abha 61411, Saudi Arabia
2   Department of Development and Operation of Oil and Gas Fields, Saint-Petersburg Mining University,
    199106 Saint-Petersburg, Russia
3   Department of Commercialization of Intellectual Activity Resultse Center for Technology Transfer of RUDN
    University, Mining Oil and Gas Department, RUDN University, 117198 Moscow, Russia
4   Department of Physics, College of Science, Imam Abdulrahman Bin Faisal University, P.O. Box 1982,
    Dammam 31441, Saudi Arabia
5   Imec-Vision Laboratory, Department of Physics, University of Antwerp, 2610 Antwerp, Belgium
6   Mining Oil and Gas Department, RUDN University, 117198 Moscow, Russia
*   Correspondence: ehsan.nazemi@uantwerpen.be

Abstract: Setting up pipelines in the oil industry is very costly and time consuming. For this reason, a pipe is usually used to transport various petroleum products, so it is very important to use an accurate and reliable control system to determine the type and amount of oil product. In this research, using a system based on the gamma-ray attenuation technique and the feature extraction technique in the frequency domain combined with a Multilayer Perceptron (MLP) neural network, an attempt has been made to determine the type and amount of four petroleum products. The implemented system consists of a dual-energy gamma source, a test pipe to simulate petroleum products, and a sodium iodide detector. The signals received from the detector were transmitted to the frequency domain, and the amplitudes of the first to fourth dominant frequency were extracted from them. These characteristics were given to an MLP neural network as input. The designed neural network has four outputs, which is the percentage of the volume ratio of each product. The proposed system has the ability to predict the volume ratio of products with a maximum root mean square error (RMSE) of 0.69, which is a strong reason for the use of this system in the oil industry.

Keywords: gamma-ray attenuation technique; Multilayer Perceptron (MLP) neural network; feature extraction; frequency domain

MSC: 97R40

1. Introduction

When different products pass through the petroleum pipeline, these products are mixed in a cross-section, which makes it difficult to recognize the type and quantity of products passing through the pipeline. Therefore, implementing a non-invasive control system to determine the type and amount of product passing through the pipe is very important. Several studies have been done to introduce non-invasive X-ray tube-based systems to determine the parameters of two-phase [1] and three-phase flows [2]. In [1], the researchers defined five time characteristics as suitable features as input of the MLP neural network for determining the type of flow regime and volumetric percentages. They stated that all flow regimes were correctly detectable, and volume percentages were predictable with a MAPE of less than 1.16, which was due to the extraction of appropriate characteristics

from the received signal. Three RBF neural networks were trained in research [2], to recognize the type of flow regimes of a three-phase flow. The inputs of these networks were frequency characteristics named the first and second dominant frequencies of the recorded signals of both detectors. The use of X-ray tubes is not limited to this, and the researchers, following the design of a control system, introduced a structure consisting of an X-ray tube, a test pipe, and a sodium iodide detector to determine the type and amount of products passing through the pipeline [3]. Due to not using feature extraction techniques, not only was a high computational load applied to the neural network, but also the introduced system was not very accurate. Following the development of the previous work [3], Balubaid et al. [4] implemented a structure similar to that in [3], but they divided the received signal into five parts of approximation and detail using wavelet transform, and approximation of the fifth stage and the details of the first to fifth stages were introduced as appropriate characteristics. In line with these researches, a research was conducted to select appropriate characteristics [5]. In this study, different time characteristics of the received signal were extracted, the most efficient of which was determined by calculating the correlation parameter between the characteristics so that the characteristics with the lowest amount of correlation were introduced as neural network input. Although the two-phase and three-phase flow parameters were detectable in the mentioned systems, in all of them, gamma-based systems are referred to as the gold standard systems. Several researches have been done to determine parameters such as the type of flow regimes and the volume percentage in two-phase [6–8] and three-phase flows [9–11]. In these researches, feature extraction techniques have not been used, but the operation of different neural networks such as MLP, RBF, adaptive neuro-fuzzy inference system, and GMDH neural network has been studied. In [12], the authors examined several time characteristics and, using an innovative method, introduced the most appropriate characteristics for determining the type of flow regimes and volumetric percentages of two-phase flows using the MLP neural network. Sattari et al. [13] used the GMDH neural network, which is a self-organized network, to select the appropriate characteristic automatically. Finally, they can classify all flow regimes correctly and predict volume percentages with a maximum RMSE of 1.11. Roshani et al. [14] applied characteristics such as count under Compton continuum and under photopeak to determine volume percentages. Using GMDH neural network, they were able to determine the volume percentage with an RMSE of less than 2.71. The deposition scale layer inside the pipe is undeniable over time that can have a significant impact on the oil industry equipment. Therefore, in [15], the researchers try to obtain the scale thickness how a two-phase flow passes through the pipe in different volume percentages and three flow regimes of annular, homogeneous, and stratified. They considered the characteristics of counts under photopeak of Ba-133 and Cs-137 as the input of the RBF neural network, and the output of the network was the thickness of scale in the pipe in millimeters. A gamma-ray attenuation-based control system was implemented in study [16]. In this study, a dual-energy source and a detector were used to determine the type and amount of product passing through the pipe. The weakness of this study was the lack of feature extraction techniques that imposed a high computational load on the network and reduced the accuracy of the proposed system. Non-iterative SGTM neural-like structure can also be useful in determining the parameters of oil industry detection systems [17,18]. In [19], a research has been done on the determination of volume ratio. In the mentioned researches, due to the lack of extraction of effective characteristics, not only relatively high accuracy has not been achieved, but also researchers have been forced to use more detectors, which increases the cost and complexity of the detection system. In the current research, using the frequency characteristics of the received signals, despite the increase in accuracy in the presented system, only one detector has been used, which has reduced the complexity of the detection system and reduced the design cost. The contributions of the current research are as follows:

1. Examining the received signals in the frequency domain and extracting appropriate characteristics.

2. The use of a detector in the structure of the control system.
3. The use of only one neural network to determine volume rates, which is due to the extraction of appropriate characteristics. This is despite the fact that in previous researches, researchers implemented separate neural networks according to the number of output parameters, which increases the cost of calculations.
4. Increasing accuracy in determining volume rates.

The current paper is structured as follows. In the second section, the simulated structure is explained in detail. Then, the received signals are transferred to the frequency domain using the Fast Fourier transform, and the frequency characteristics are extracted from them. In the next section, the obtained characteristics are used as inputs of the MLP neural network and volume ratio are predicted. In Section 5, the results of this research are stated and the conclusion is presented in the last section.

2. Simulation Setup

Ethylene glycol, crude oil, gasoline, and gasoil have been studied in this study as by-products. The density of these products is 1.114, 0.975, 0.721, and 0.826 g/cm^3, respectively. In this research, a test pipe is considered with an external diameter of 10 cm and a thickness of 0.25 cm. The detection system consists of a dual-energy gamma source, consisting of americium-241 and barium-133, and a sodium iodide (NaI) detector located on either side of the test pipe. The distance between the source and the detector is 30 cm. The simulated structure is shown in Figure 1. This simulation is done with version X of Monte Carlo N Particle code (MCNP-X). First, one product is placed inside the pipe in a single phase, and then the next product is loaded into the pipe. The two products overlap in a cross-section, and over time the amount of the first product decreases, and the second product increases. In this simulation, all possible modes for combining two by two petroleum by-products in volume percentages of 5% to 95% with steps of 5% are implemented. A total of 118 simulations, including 6 different modes × 19 different volume percentages + 4 single-phase modes, are carried out. The received signals can be seen for several different modes in Figure 2. The simulated structure and sample of the signal received by the detector are shown in Figure 1. The reproduction aftereffects of this study have been approved by past examinations [6].
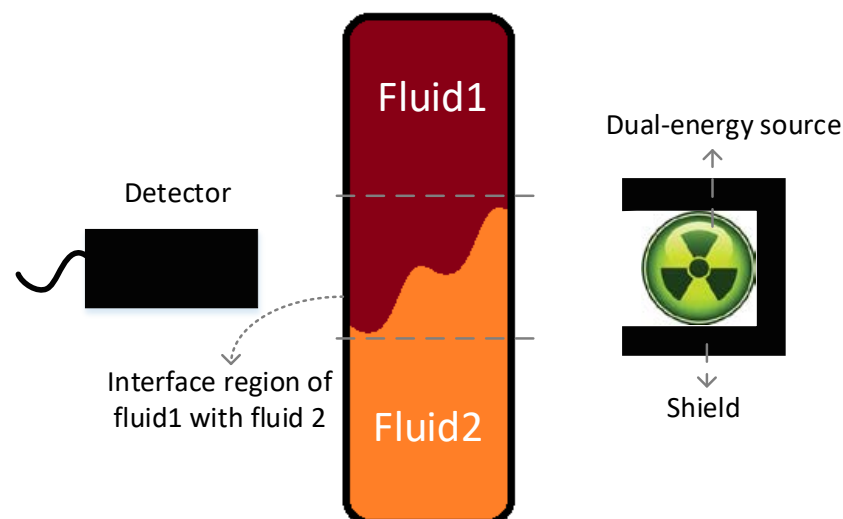
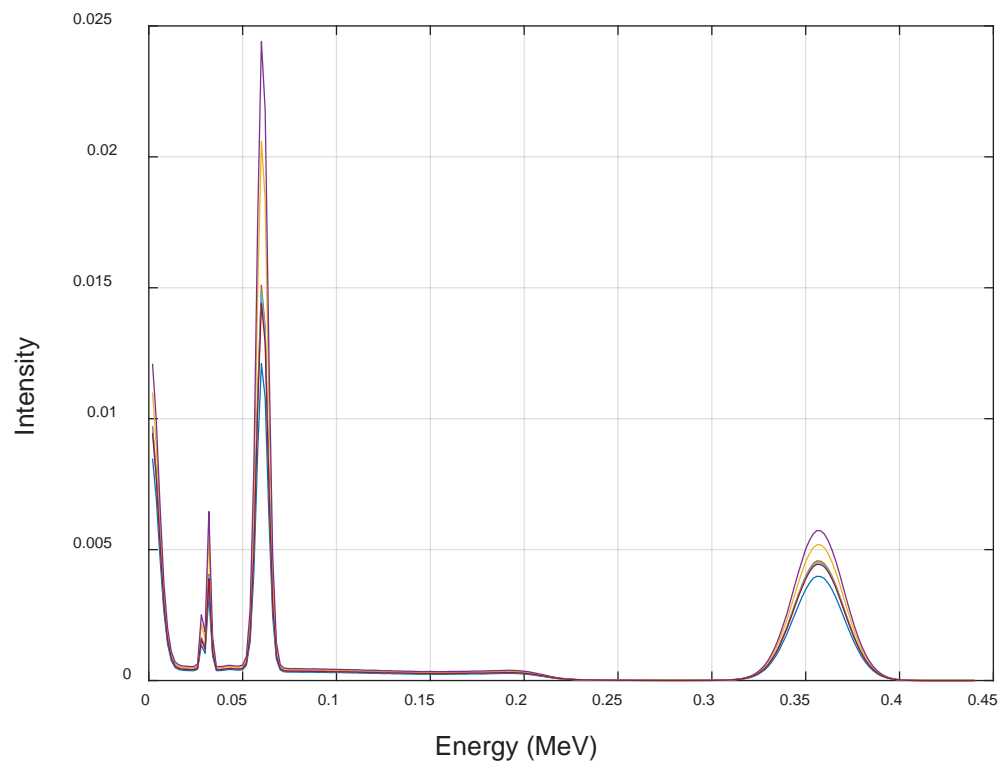

Figure 1. Simulation structure.

Figure 2. Recorded spectrum by the detector.

According to the Beer–Lambert law, the attenuation rate of a narrow gamma-ray beam is as follows

$$I = I_0 e^{-\mu \rho x} \tag{1}$$

where I is the intensity of un-collided and primary photons is represented by I_0. The mass attenuation coefficient and density of absorber material are shown by μ and ρ, respectively. x is the beam path length through the absorber. Equation (1) states that gamma rays have different attenuation rates when they hit different objects. This difference in the attenuation rate can be a very important factor to determine the type and amount in many detection systems.

3. Frequency Feature Extraction

The signals received from the detector are large and require to feature extraction for better interpretation to prepare for neural network training. There are several methods for extracting signal characteristics, including extraction of time, frequency, and time-frequency characteristics. In this study, the frequency characteristics of the received signals are investigated. For this purpose, to transmit the signal from the time domain to the frequency, the Fast Fourier Transform (FFT) is used according to the following Equation (2).

$$Y(k) = \sum_{J=1}^{n} \times (J) w_n^{(y-1)(k-1)} \tag{2}$$

where Y(k) = FFT(X) and $w_n = e^{(-2\pi i)/n}$ is one of the n roots of unity.

From the frequency domain signals, the amplitude of the first to the fourth dominant frequency were extracted and introduced as neural network inputs. The extracted features have been introduced as very useful features in previous researches [20–22], so the mentioned characteristics have been used in order to increase the accuracy of the volumetric rate detection system. The frequency domain signal and the extracted characteristics are shown in Figure 3.
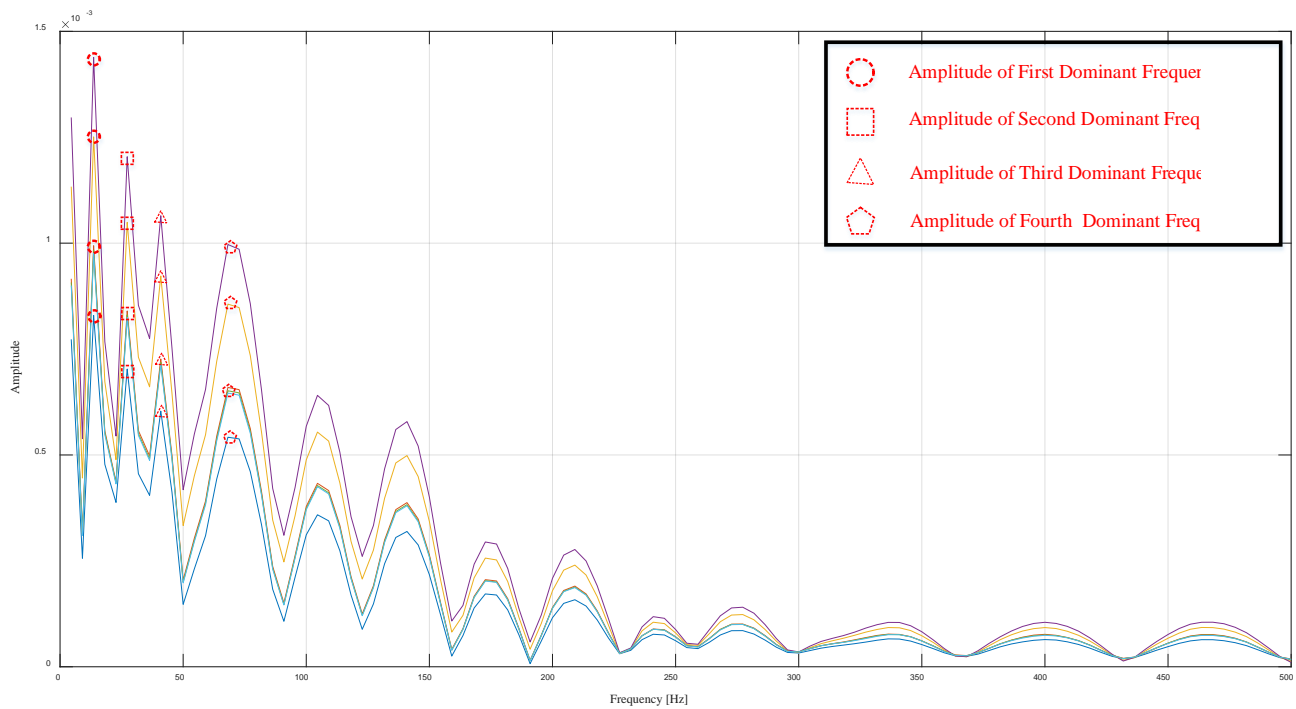
Figure 3. Frequency domain signal and extracted characteristics.

4. The Multilayer Perceptron Neural Network

The human brain has millions of computing units called neurons. All these neurons are connected with each other. Neurons have branches called dendrites that receive information from other neurons. The nucleus is the processing unit of the neuron, which after processing the received information, transmits the output information to other neurons through the output cable called the axon. All these processes happen in the physiological and biochemical fields. Researchers have proposed several methods to model this function in mathematics, one of the most common of which is the MLP neural network. The structure of this network has an input layer and an output layer. There can be different number of hidden layers between these two layers. In the hidden layers, a series of mathematical processes are performed, which are introduced as the activation function. The number of these layers, the number of neurons in the hidden layers, and the type of activation function depend on the nature and degree of non-linearity of the available data. In the implementation of neurons mathematically, the output of neurons is as follows [23,24].

$$n_l = \sum_{i=1}^{u} x_i w_{ij} + b \quad j = 1, 2, \cdots, m \tag{3}$$

$$u_j = f\left(\sum_{i=1}^{u} x_i w_{ij} + b\right) \quad j = 1, 2, \cdots, m \tag{4}$$

$$output = \sum_{n=1}^{j} (u_n w_n) + b \tag{5}$$

In which x presents the input parameters; the bias term, the weighting factor, and the activation function are shown with b, w, and f, respectively. The index i is the input number, and j is the neuron number in every hidden layer. In recent years, different mathematical approaches have been used for analyzing data in plenty of engineering fields [25–48], but it has been proved that Artificial Neural network (ANN) is the most powerful tool for estimation and classification. For the implementation of neural networks, the collected data are usually divided into three categories: training data, validation data, and test data.

Training data usually contain 70% of the data. The neural network is designed based on this data, and the network fits on these data. A total of 15% of the data are allocated to validation data. These data are used for testing during training. Although the neural network is not trained with this data, it is essential to prevent over-fitting and under-fitting problems. The rest of the data fall into the category of test data. After completing the network design steps, these data are given to the neural network input to check the network performance against data that have not been seen before. Proper network performance against these three datasets guarantees network performance in operating conditions. To extract the mentioned characteristics and train the MLP neural network, MATLAB software was applied. Although there are many toolboxes for neural network training in this software, no pre-designed toolbox was used in this research and all steps of neural network implementation are programmed for more freedom of action. In the implementation stages, the 'newff' function was used for training the MLP neural network. In order to prevent over-fitting and under-fitting of the neural network and to ensure the proper functioning of the designed neural network, the available data are divided into three sub-data. The first sub-data are the training data, which includes the majority of the data. These data are used to train the neural network. The network is fitted using these data. The second sub-data are the validation data used for testing during training. The correct response of the neural network to this dataset shows the correct training process. After the implementation of the neural network, the designed network is evaluated against the test sub-data. The neural network has not seen these data and is not trained with them, and it is only used to check the performance of the neural network. The accurate response of the neural network to these three datasets guarantees the proper functioning of the neural network in operational conditions and the absence of over-fitting and under-fitting problems.

5. Result and Discussion

An MLP neural network with four inputs and four outputs was designed that the inputs of this network are the characteristics of the amplitude of the first to fourth dominant frequency. Of the 118 available data, 82 were allocated to training data, 18 to validation data, and 18 to test data. The outputs of this network include the percentage of volume ratio of each of the petroleum by-products. It is important to say that neural networks with the different of number layers and different neurons in each layer have been implemented and tested, and a the best structure is shown in Figure 4. The target outputs can be predicted with fewer layers, but their accuracy is not high, and since the aim of this research is to increase the accuracy in determining volume ratio, a structure that has the least error has been presented. Regression and error diagrams have been used to show the performance of this network. The high compatibility of the stars and line indicates the high accuracy of the designed network. The amount of error between the network output data and the desired output data can be seen in the error diagram. The performance of the network for determining the volume percentage of ethylene glycol, crude oil, gasoline, and gasoil are shown in Figures 5–8, respectively. To calculate the amount of network error, two criteria, mean square error (MSE) and root mean square error (RMSE), have been computed with Equations (5) and (6). The accuracy of the network and the structure of the designed network are shown in Table 1.

$$\text{MSE} = \frac{\sum_{j=1}^{N}\left(X_j(\text{Exp}) - X_j(\text{Pred})\right)^2}{N} \tag{6}$$

$$\text{RMSE} = \left[\frac{\sum_{j=1}^{N}\left(X_j(\text{Exp}) - X_j(\text{Pred})\right)^2}{N}\right]^{0.5} \tag{7}$$
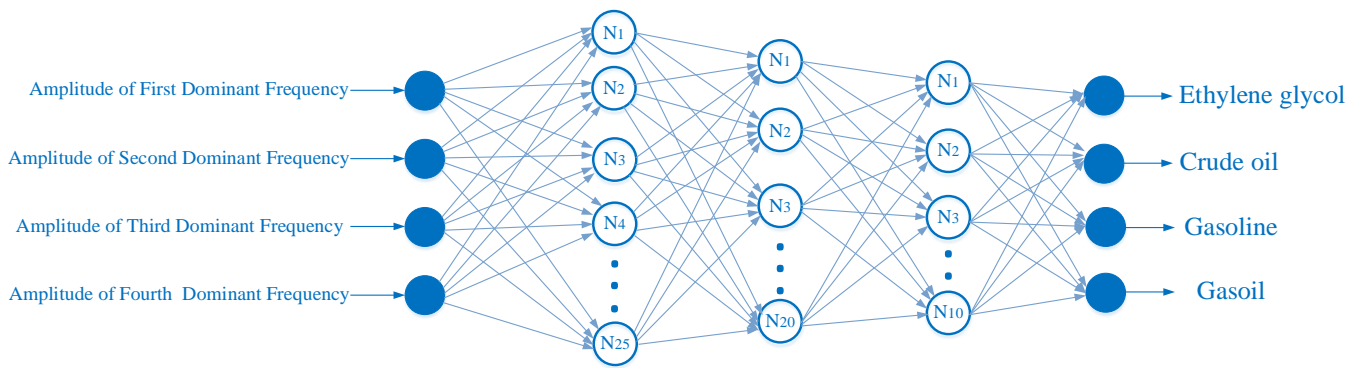
Figure 4. Implemented MLP neural network.
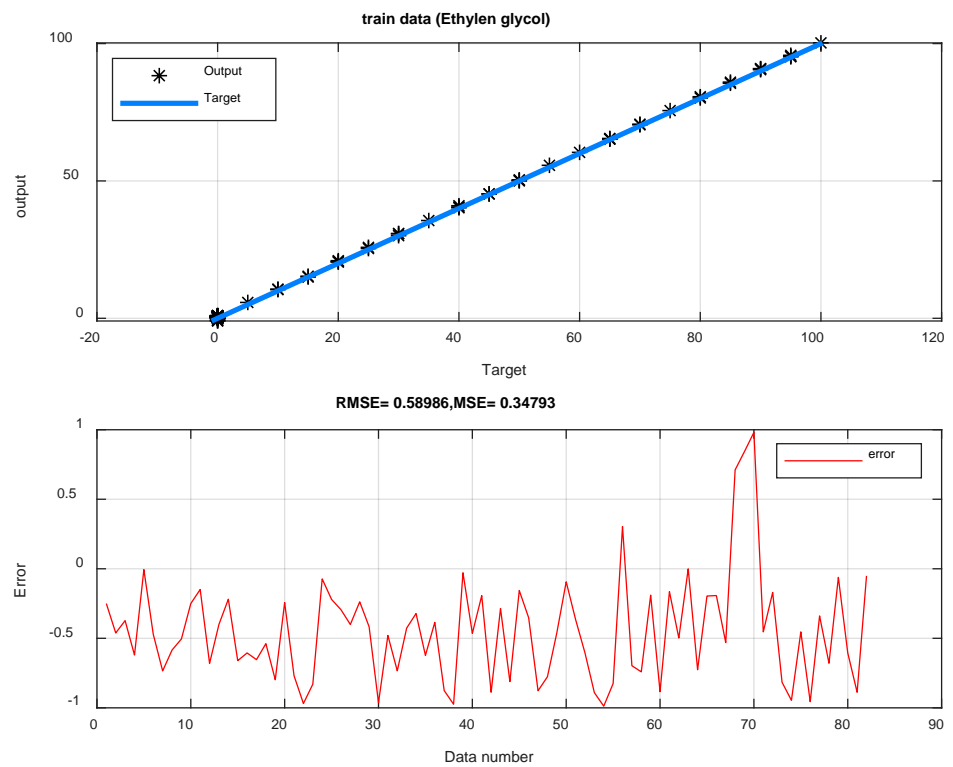
(a)

Figure 5. *Cont.*
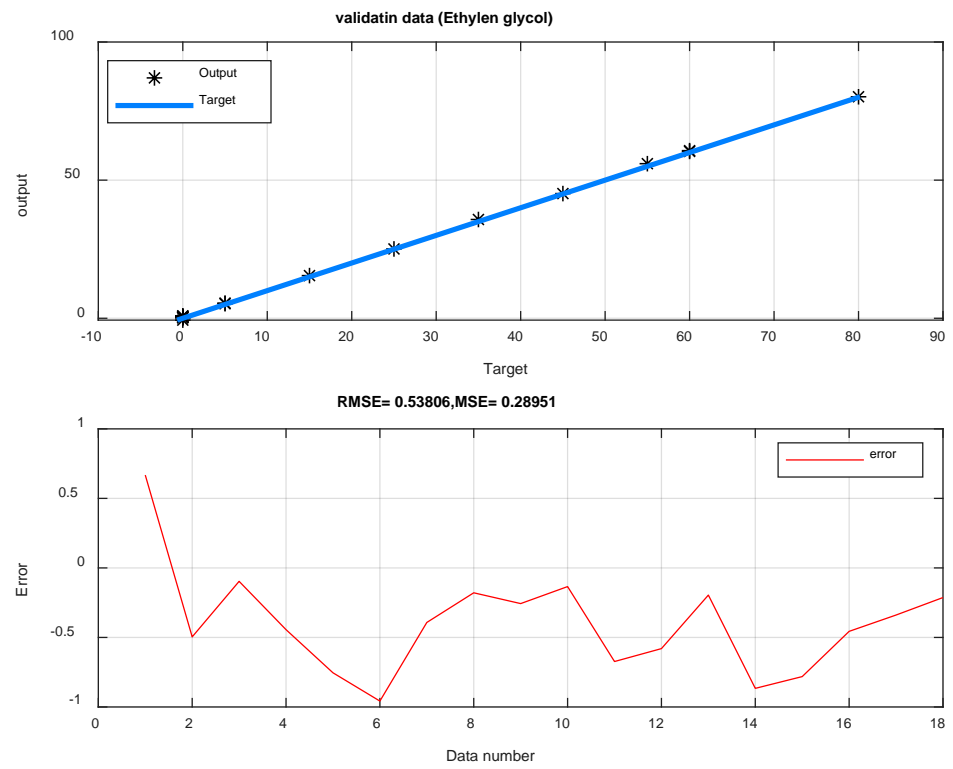
(**b**)
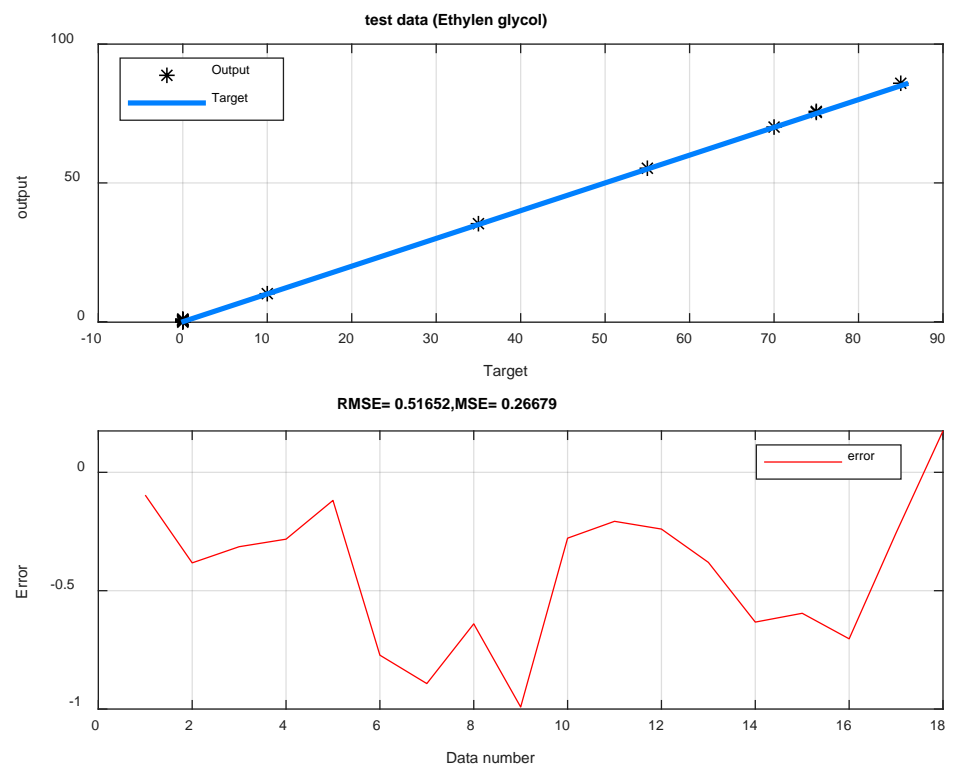
(**c**)

Figure 5. Network performance for predicting the volume rate of ethylene glycol (**a**) Training, (**b**) validation, and (**c**) testing dataset.

(**a**)

(**b**)

Figure 6. *Cont.*

(**c**)
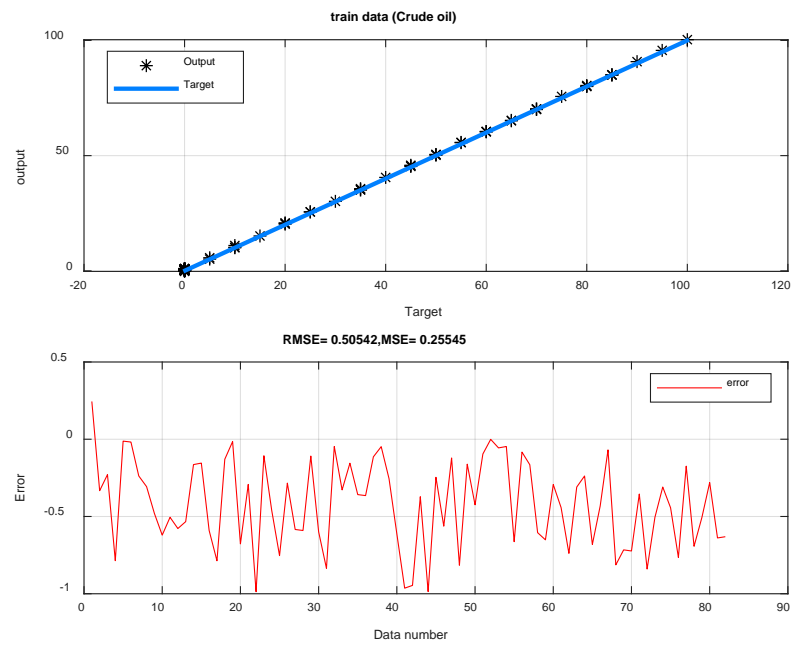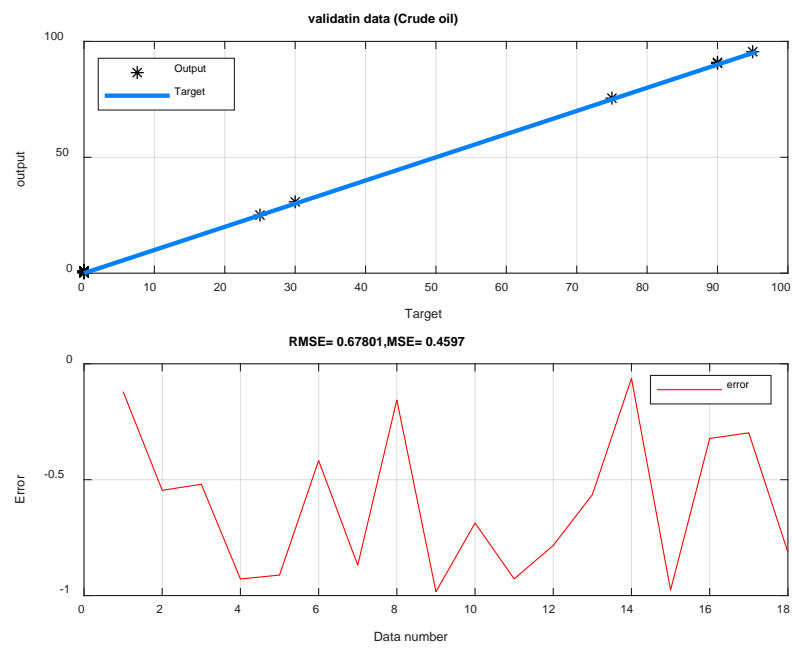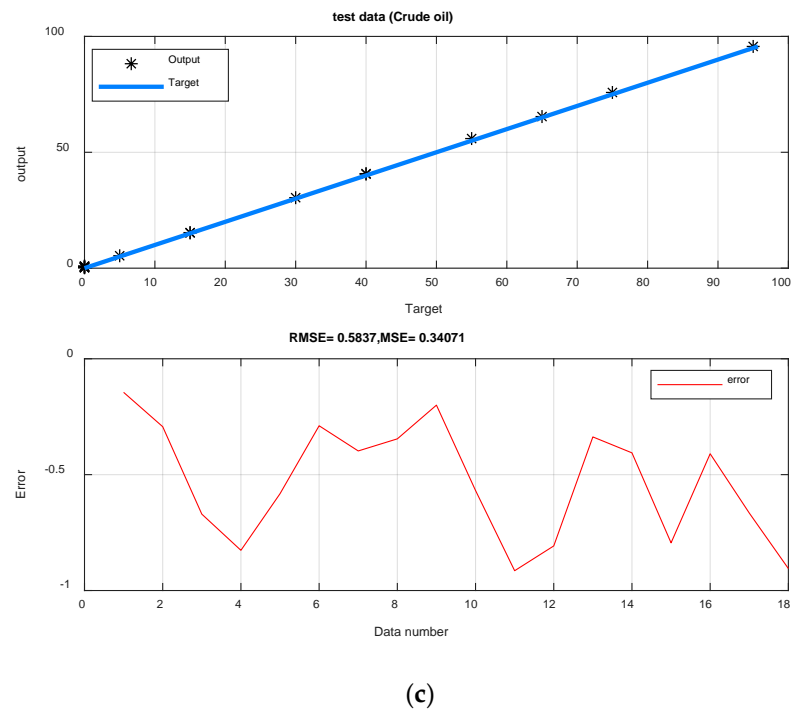
Figure 6. Network performance for predicting the volume rate of crude oil: (**a**) training, (**b**) validation, and (**c**) testing dataset.

(**a**)
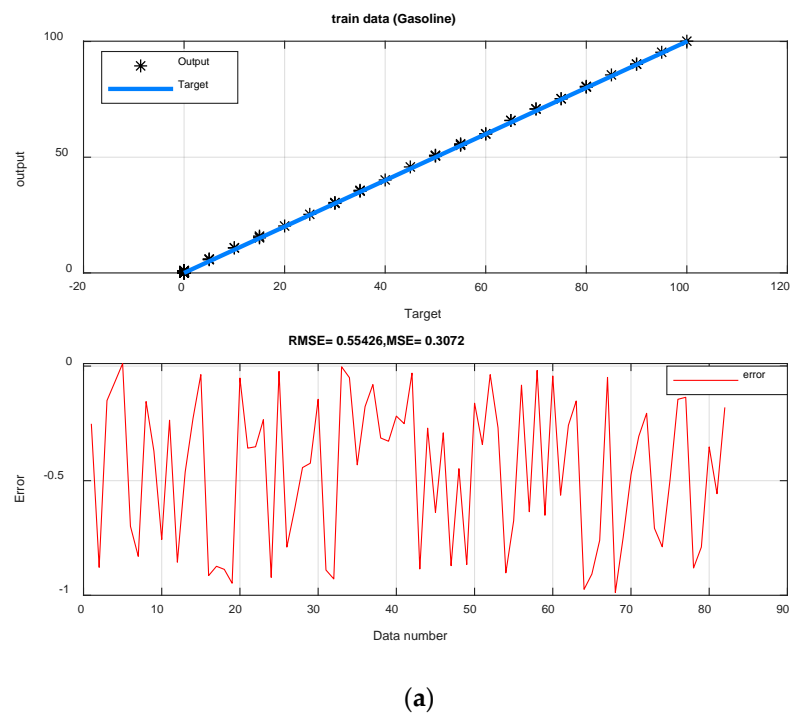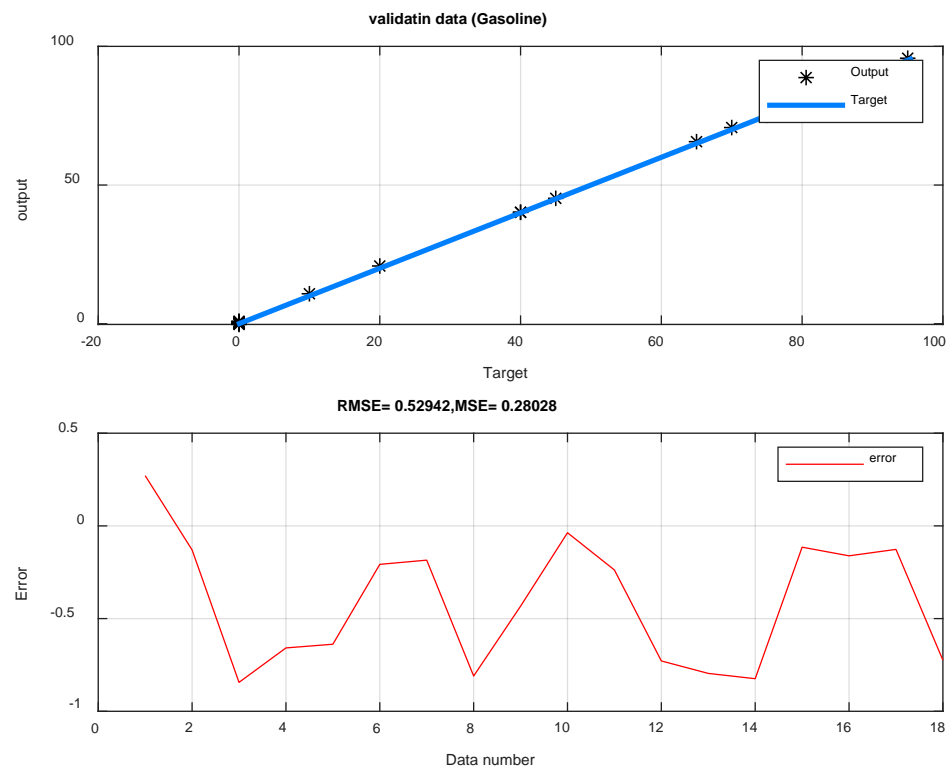
Figure 7. *Cont.*

(b)
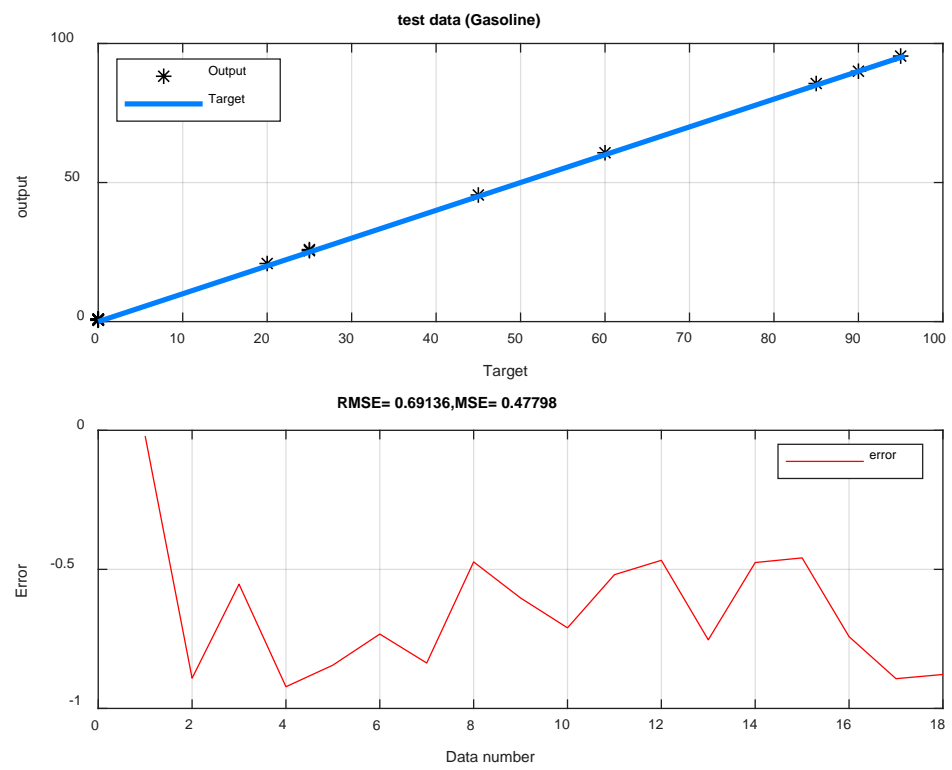
(c)

Figure 7. Network performance for predicting the volume rate of gasoline: (**a**) training, (**b**) validation, and (**c**) testing dataset.

(**a**)

(**b**)

Figure 8. *Cont.*

(**c**)
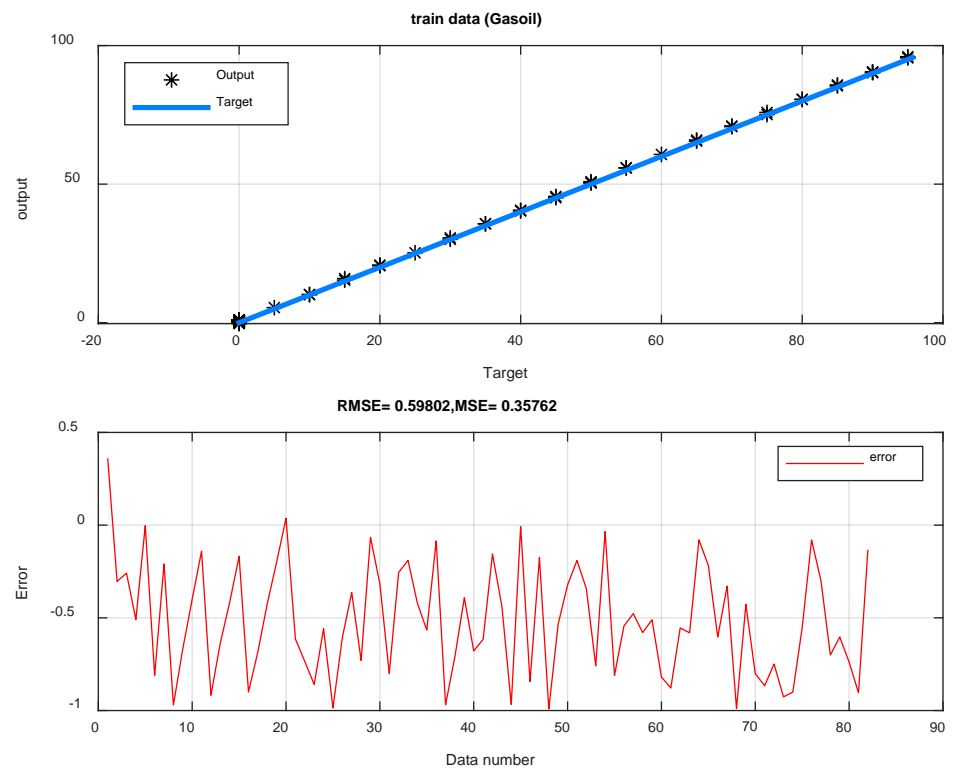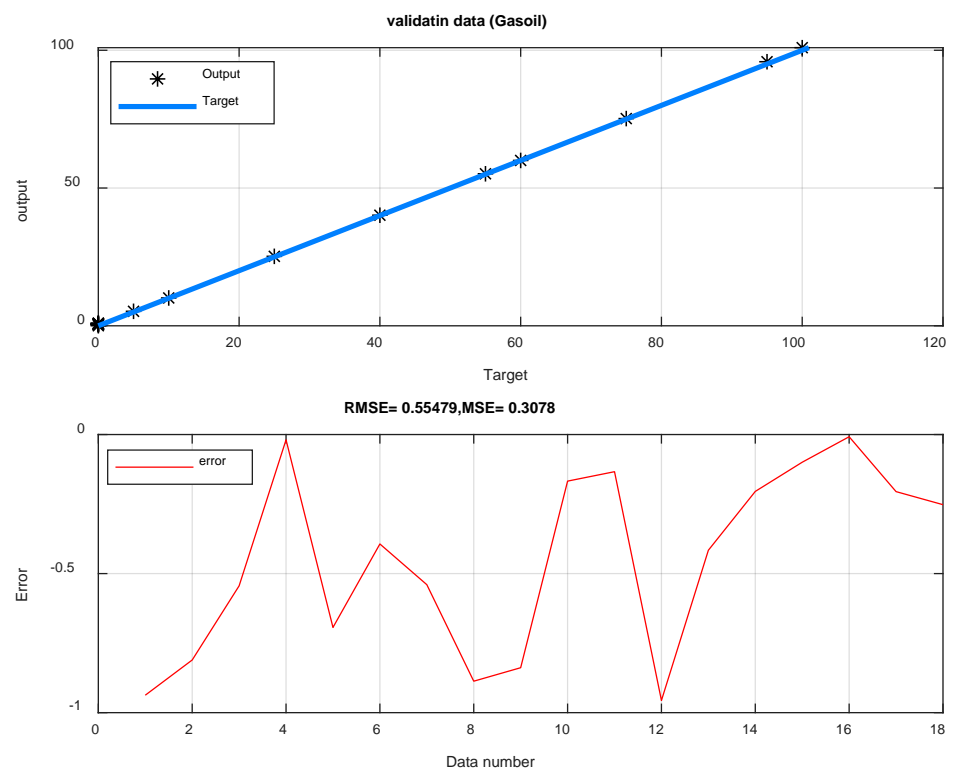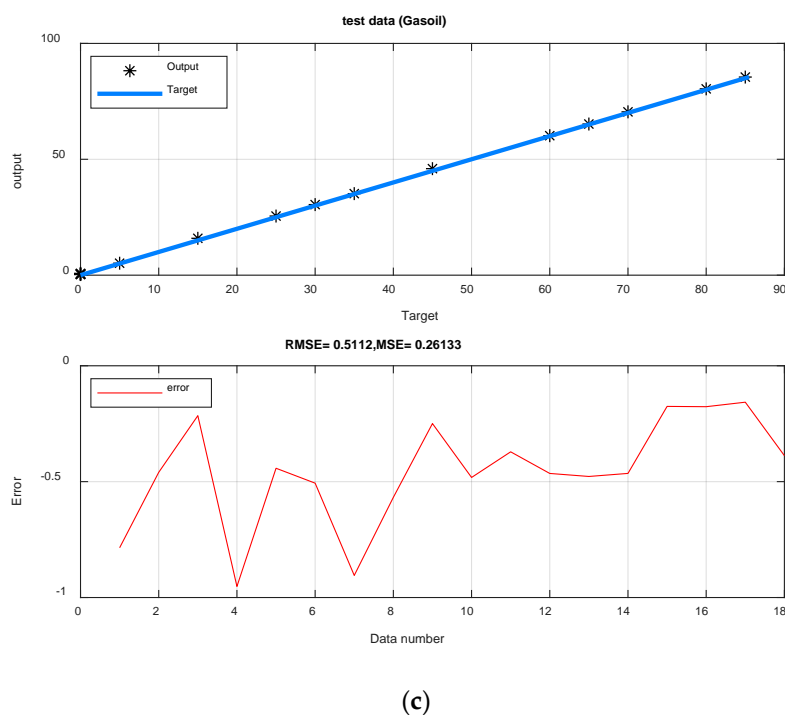
Figure 8. Network performance for predicting the volume rate of gasoil: (**a**) training, (**b**) validation, and (**c**) testing dataset.

Table 1. The characteristics of designed networks.

ANN	MLP		
No. of neurons in the input layer	4		
No. of neurons in the 1st hidden layer	25		
No. of neurons in the 2nd hidden layer	20		
No. of neurons in the 3rd hidden layer	10		
No. of neurons in the output layer	4		
No. of epoch	850		
Hidden neuron activation function	Tansig		
MSE of predicting ethylene glycol	**Training data**	**Validation data**	**Test data**
	0.34	0.28	0.26
RMSE of predicting ethylene glycol	0.58	0.53	0.51
MSE of predicting crude oil	0.25	0.45	0.34
RMSE of predicting crude oil	0.50	0.67	0.58
MSE of predicting gasoline	0.30	0.28	0.45
RMSE of predicting gasoline	0.55	0.52	0.67
MSE of predicting gasoil	0.41	0.30	0.26
RMSE of predicting gasoil	0.66	0.55	0.51

Appropriate inputs in this study have been obtained by extracting frequency features. The use of these features, in addition to increasing the accuracy of the proposed system, reduces the volume of calculations. Using only one neural network with four outputs, the volume percentages of each product could be predicted with high accuracy, while more neural networks were needed in previous studies [1–5] to determine the volume percentage of each product used. The target outputs and the outputs in the designed neural network are shown in Table 2. The accuracy of the introduced detection system is compared with the previous research in Table 3. The general process of the current research is shown in Figure 9. According to this figure, the detection process is that first, four petroleum products were simulated two by two with each other in different volume percentages in a test pipe. A dual-energy gamma source and a NaI detector were placed on both sides of this

pipe, and data related to each simulation were collected and labeled. Then, using FFT, the received signals were transferred to the frequency domain and the frequency characteristics were extracted from them. Finally, the extracted characteristics were used to train a neural network, which its output was the volume rate of petroleum products.

Step 1: Simulating the structure of the detection system
Ethylene glycol ,crude oil ,gasoline ,and gasoil have been studied in this study as by-products. A total of 118 simulations, including 6 different modes × 19 different volume percentages + 4 single-phase modes, are carried out.

Step 2: Data collection
In this simulation, all possible modes for combining two by two petroleum by-products in volume percentages of 5% to 95% with steps of 5% are implemented.

Step3: Feature extraction
The signals received from the detector are large and require to feature extraction for better interpretation to prepare for neural network training .In this study ,the frequency characteristics of the received signals are investigated .From the frequency domain signals ,the amplitude of the first to the fourth dominant frequency were extracted and introduced as neural network inputs .

Step 4: MLP neural network
An MLP neural network with four inputs and four outputs was designed that the inputs of this network are the characteristics of the amplitude of the first to fourth dominant frequency .Of the118 available data82 ,were allocated to training data18 ,to validation data ,and18 to test data .The outputs of this network include the percentage of volume ratio of each of the petroleum by-products.

Figure 9. The general process of the research to determine the volumetric ratio of petroleum products.

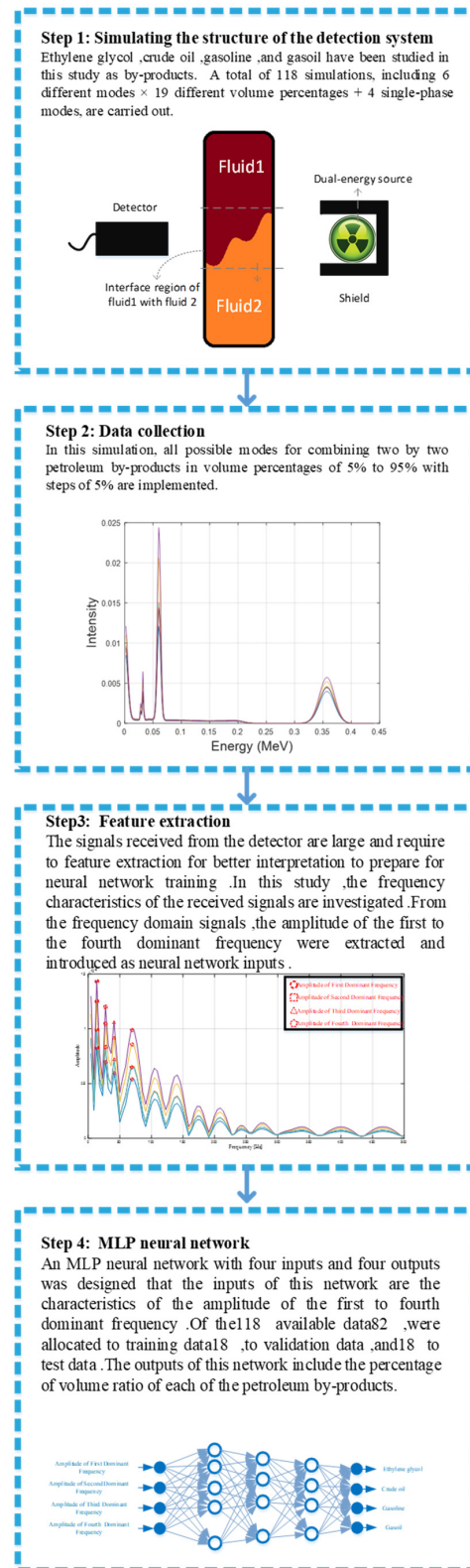**Table 2.** Comparison of target values with neural network outputs.

Ethylene Glycol				Crude Oil				Gasoline				Gasoil			
Train		Validation		Train		Validation		Train		Validation		Train		Validation	
Target	Output	Target	Output	Target	Output	Target	Output	Target	Output	Target	Output	Target	Output	Target	Output
100	100.2503	0	−0.6679	0	−0.2444	0	0.1200	0	0.2518	0	−0.2710	0	−0.3601	100	100.9374
0	0.4616	5	5.4959	100	100.3333	95	95.5458	0	0.8781	0	0.1298	0	0.3037	0	0.8107
0	0.3729	25	25.0965	0	0.2291	75	75.5199	100	100.1504	0	0.8440	0	0.2588	0	0.5440
10	10.6204	15	15.4440	90	90.7862	0	0.9285	0	0.0703	85	85.6582	0	0.5093	0	0.0190
15	15.0060	35	35.7542	85	85.0123	0	0.9116	0	−0.0111	65	65.6383	0	0.0029	0	0.6936
20	20.4711	55	55.9576	80	80.0183	0	0.4176	0	0.6988	45	45.2076	0	0.8107	0	0.3935
30	30.7347	60	60.3923	70	70.2377	0	0.8690	0	0.8302	40	40.1848	0	0.2093	0	0.5399
35	35.5848	80	80.1789	65	65.3069	0	0.1560	0	0.1548	20	20.8099	0	0.9703	0	0.8869
40	40.5047	5	5.2565	60	60.4803	0	0.9834	0	0.3711	0	0.4331	0	0.6670	95	95.8385
45	45.2502	45	45.1342	55	55.6207	0	0.6872	0	0.7567	0	0.0370	0	0.4000	55	55.1675
50	50.1489	60	60.6732	50	50.5052	0	0.9281	0	0.2362	0	0.2378	0	0.1402	40	40.1336
55	55.6802	0	0.5803	45	45.5780	30	30.7838	0	0.8557	70	70.7285	0	0.9178	0	0.9562
60	60.3997	0	0.1954	40	40.5334	90	90.5645	0	0.4622	10	10.7957	0	0.6351	0	0.4161
65	65.2189	0	0.8662	35	35.1642	25	25.0627	0	0.2284	0	0.8243	0	0.4157	75	75.2045
70	70.6607	0	0.7815	30	30.1545	90	90.9765	0	0.0372	0	0.1148	0	0.1682	10	10.0996
75	75.6053	0	0.4562	25	25.5907	0	0.3221	0	0.9140	40	40.1615	0	0.8996	60	60.0079
80	80.6537	0	0.3388	20	20.7869	0	0.2980	0	0.8735	75	75.1267	0	0.6834	25	25.2053
85	85.5384	0	0.2130	15	15.1296	0	0.8131	0	0.8869	95	95.7242	0	0.4242	5	5.2522
90	90.7981	**Test**		10	10.0152	**Test**		0	0.9475	**Test**		0	0.1989	**Test**	
95	95.2433	Target	Output	5	5.6774	Target	Output	0	0.0524	Target	Output	0	−0.0373	Target	Output
5	5.7691	10	10.0963	0	0.2924	0	0.1449	95	95.3581	90	90.0206	0	0.6137	0	0.7854
20	20.9692	75	75.3825	0	0.9871	0	0.2932	80	80.3520	25	25.8914	0	0.7352	0	0.4598
25	25.8302	35	35.3142	0	0.1070	0	0.6704	75	75.2338	0	0.5532	0	0.8594	65	65.2154
30	30.0729	55	55.2824	0	0.4603	0	0.8266	70	70.9220	0	0.9220	0	0.5587	45	45.9522
40	40.2206	70	70.1186	0	0.7534	0	0.5823	60	60.0233	0	0.8444	0	0.9862	30	30.4423
45	45.2943	75	75.7724	0	0.2841	0	0.2891	55	55.7898	0	0.7327	0	0.6064	25	25.5066
50	50.4005	85	85.8925	0	0.5841	0	0.3978	50	50.6236	0	0.8367	0	0.3638	15	15.9047
65	65.2375	0	0.6401	0	0.5907	5	5.3456	35	35.4429	95	95.4732	0	0.7297	0	0.5678
70	70.4170	0	0.9915	0	0.1090	15	15.2002	30	30.4238	85	85.6029	0	0.0655	0	0.2494
85	85.9635	0	0.2781	0	0.5994	40	40.5686	15	15.1449	60	60.7102	0	0.3174	0	0.4820
90	90.4796	0	0.2070	0	0.8356	55	55.9146	10	10.8898	45	45.5192	0	0.7994	0	0.3714
95	95.7340	0	0.2397	0	0.0471	75	75.8077	5	5.9287	25	25.4674	0	0.2552	0	0.4647

Table 2. *Cont.*

| Ethylene Glycol | | | | Crude Oil | | | | Gasoline | | | | Gasoil | | | |
| Train | | Validation | | Train | | Validation | | Train | | Validation | | Train | | Validation | |
Target	Output	Target	Output	Target	Output	Target	Output	Target	Output	Target	Output	Target	Output	Target	Output
10	10.4268	0	0.3804	0	0.3282	15	15.3373	0	0.0031	0	0.7534	90	90.1902	85	85.4777
15	15.3218	0	0.6327	0	0.1551	30	30.4061	0	0.0505	0	0.4754	85	85.4217	70	70.4645
20	20.6227	0	0.5955	0	0.3584	40	40.7944	0	0.4310	0	0.4587	80	80.5661	60	60.1754
25	25.3852	0	0.7034	0	0.3649	65	65.4100	0	0.1768	0	0.7419	75	75.0850	35	35.1766
30	30.8757	0	0.2561	0	0.1140	95	95.6657	0	0.0806	0	0.8931	70	70.9688	5	5.1572
40	40.9742	0	−0.1749	0	0.0482	0	0.9053	0	0.3138	20	20.8780	60	60.7076	80	80.3878
50	50.0287	-	-	0	0.2554	-	-	0	0.3280	-	-	50	50.3917	-	-
65	65.4649	-	-	0	0.6128	-	-	0	0.2182	-	-	35	35.6784	-	-
80	80.1930	-	-	0	0.9640	-	-	0	0.2512	-	-	20	20.6160	-	-
90	90.8877	-	-	0	0.9461	-	-	0	0.0308	-	-	10	10.1557	-	-
95	95.2856	-	-	0	0.3720	-	-	0	0.8852	-	-	5	5.4375	-	-
0	0.8116	-	-	10	10.9860	-	-	90	90.2708	-	-	0	0.9674	-	-
0	0.1563	-	-	20	20.2464	-	-	80	80.6384	-	-	0	0.0074	-	-
0	0.3523	-	-	25	25.5626	-	-	75	75.2913	-	-	0	0.8436	-	-
0	0.8774	-	-	35	35.1213	-	-	65	65.8709	-	-	0	0.1757	-	-
0	0.7764	-	-	45	45.8156	-	-	55	55.4477	-	-	0	0.9914	-	-
0	0.4610	-	-	50	50.1615	-	-	50	50.8660	-	-	0	0.5332	-	-
0	0.0937	-	-	60	60.4247	-	-	40	40.1619	-	-	0	0.3229	-	-
0	0.3649	-	-	65	65.0956	-	-	35	35.3425	-	-	0	0.1906	-	-
0	0.6050	-	-	70	70.0008	-	-	30	30.0373	-	-	0	0.3430	-	-
0	0.8907	-	-	80	80.0561	-	-	20	20.2694	-	-	0	0.7588	-	-
0	0.9881	-	-	85	85.0471	-	-	15	15.9021	-	-	0	0.0350	-	-
0	0.8255	-	-	95	95.6633	-	-	5	5.6746	-	-	0	0.8099	-	-
0	−0.3040	-	-	5	5.0832	-	-	0	0.0832	-	-	95	95.5449	-	-
0	0.6973	-	-	10	10.1651	-	-	0	0.6355	-	-	90	90.4770	-	-
0	0.7413	-	-	20	20.6047	-	-	0	0.0190	-	-	80	80.5796	-	-
0	0.1897	-	-	35	35.6512	-	-	0	0.6508	-	-	65	65.5103	-	-
0	0.8841	-	-	45	45.2931	-	-	0	0.0432	-	-	55	55.8189	-	-
0	0.1644	-	-	50	50.4422	-	-	0	0.5633	-	-	50	50.8786	-	-
0	0.4981	-	-	55	55.7387	-	-	0	0.2583	-	-	45	45.5543	-	-
0	0.0006	-	-	60	60.3096	-	-	0	0.1521	-	-	40	40.5810	-	-
0	0.7261	-	-	70	70.2379	-	-	0	0.9742	-	-	30	30.0793	-	-

Table 2. *Cont.*

| Ethylene Glycol | | | | Crude Oil | | | | Gasoline | | | | Gasoil | | | |
| Train | | Validation | | Train | | Validation | | Train | | Validation | | Train | | Validation | |
Target	Output	Target	Output	Target	Output	Target	Output	Target	Output	Target	Output	Target	Output	Target	Output
0	0.1960	-	-	75	75.6808	-	-	0	0.9075	-	-	25	25.2178	-	-
0	0.1926	-	-	80	80.4320	-	-	0	0.7600	-	-	20	20.6035	-	-
0	0.5311	-	-	85	85.0690	-	-	0	0.0494	-	-	15	15.3289	-	-
0	−0.7112	-	-	0	0.8132	-	-	5	5.9879	-	-	95	95.9897	-	-
0	−0.8436	-	-	0	0.7161	-	-	10	10.7479	-	-	90	90.4273	-	-
0	−0.9808	-	-	0	0.7233	-	-	15	15.4751	-	-	85	85.8016	-	-
0	0.4536	-	-	0	0.3547	-	-	25	25.3062	-	-	75	75.8660	-	-
0	0.1702	-	-	0	0.8403	-	-	30	30.2059	-	-	70	70.7492	-	-
0	0.8165	-	-	0	0.5051	-	-	35	35.7077	-	-	65	65.9260	-	-
0	0.9459	-	-	0	0.3093	-	-	45	45.7886	-	-	55	55.9010	-	-
0	0.4537	-	-	0	0.4437	-	-	50	50.4946	-	-	50	50.5521	-	-
0	0.9560	-	-	0	0.7649	-	-	55	55.1449	-	-	45	45.0799	-	-
0	0.3390	-	-	0	0.1744	-	-	60	60.1362	-	-	40	40.3001	-	-
0	0.6794	-	-	0	0.6930	-	-	65	65.8811	-	-	35	35.7006	-	-
0	0.0618	-	-	0	0.5073	-	-	70	70.7896	-	-	30	30.6033	-	-
0	0.6051	-	-	0	0.2804	-	-	80	80.3527	-	-	20	20.7391	-	-
0	0.8882	-	-	0	0.6390	-	-	85	85.5569	-	-	15	15.9040	-	-
0	0.0510	-	-	0	0.6310	-	-	90	90.1803	-	-	10	10.1328	-	-

Table 3. The accuracy of the presented detection system compared to previous research.

Ref	Extracted Features	Type of Neural Network	MSE		RMSE	
			Training	Testing	Training	Testing
[12]	Time domain	GMDH	1.24	1.20	1.11	1.09
[13]	Time domain	MLP	0.21	0.036	0.46	0.6
[14]	Lack of feature extraction	GMDH	7.34	4.92	2.71	2.21
[15]	Lack of feature extraction	RBF	0.049	0.37	0.22	0.19
[25]	Frequency domain	MLP	0.17	0.67	0.42	0.82
[26]	Lack of feature extraction	MLP	2.56	2.56	1.6	1.6
[current study]	**Frequency domain**	**MLP**	0.41	0.45	0.66	0.67

6. Conclusions

Implementing an oil pipeline control system is very important to determine the amount and type of product in the pipeline. The proposed control system consists of a dual-energy source of gamma and one detector located on either side of a pipe. There are four petroleum products called ethylene glycol, crude oil, gasoil, and gasoline inside the pipe, which were examined in different volume ratios. Investigating the frequency characteristics of the received signals by the detector were on the agenda. The characteristics of the amplitude of the first to fourth dominant frequency were extracted from the signal and defined as the input of the artificial neural network. The designed MLP network has four outputs, each of which is related to the volume ratio of each product. By obtaining all four outputs, the amount and type of product passing through the pipeline can be obtained. The maximum RMSE of the designed neural network to determine the volume ratio was 0.67, which is a very small value, compared to the detection systems of previous researches. The major limitation of this research is working with radioisotope devices, which requires the use of protective clothing. The high accuracy obtained from this research is due to the extraction of appropriate characteristics from the received signals, which can be investigated in future researches as inputs of different type of neural networks. In addition, the use of deep neural networks to achieve higher accuracy is strongly recommended to researchers in this field.

Author Contributions: Formal analysis, I.M.N. and I.M.I.; Funding acquisition, A.M.M.; Methodology, A.M.M., A.A.A.-Q., H.H.A. and K.S.N.; Software, H.H.A., A.A.A.-Q. and A.M.M.; Supervision, I.M.N.; Visualization, E.N., I.M.N. and I.M.I. All authors have read and agreed to the published version of the manuscript.

Institutional Review Board Statement: Not applicable.

Informed Consent Statement: Not applicable.

Data Availability Statement: Not applicable.

Conflicts of Interest: The authors declare no conflict of interest.

References

1. Basahel, A.; Sattari, M.; Taylan, O.; Nazemi, E. Application of Feature Extraction and Artificial Intelligence Techniques for Increasing the Accuracy of X-ray Radiation Based Two Phase Flow Meter. *Mathematics* **2021**, *9*, 1227. [CrossRef]
2. Taylan, O.; Sattari, M.A.; Essoussi, I.E.; Nazemi, E. Frequency Domain Feature Extraction Investigation to Increase the Accuracy of an Intelligent Nondestructive System for Volume Fraction and Regime Determination of Gas-Water-Oil Three-Phase Flows. *Mathematics* **2021**, *9*, 2091. [CrossRef]
3. Roshani, G.H.; Ali, P.J.M.; Mohammed, S.; Hanus, R.; Abdulkareem, L.; Alanezi, A.A.; Sattari, M.A.; Amiri, S.; Nazemi, E.; Eftekhari-Zadeh, E.; et al. Simulation Study of Utilizing X-ray Tube in Monitoring Systems of Liquid Petroleum Products. *Processes* **2021**, *9*, 828. [CrossRef]
4. Balubaid, M.; Sattari, M.A.; Taylan, O.; Bakhsh, A.A.; Nazemi, E. Applications of Discrete Wavelet Transform for Feature Extraction to Increase the Accuracy of Monitoring Systems of Liquid Petroleum Products. *Mathematics* **2021**, *9*, 3215. [CrossRef]
5. Mayet, A.M.; Alizadeh, S.M.; Nurgalieva, K.S.; Hanus, R.; Nazemi, E.; Narozhnyy, I.M. Extraction of Time-Domain Characteristics and Selection of Effective Features Using Correlation Analysis to Increase the Accuracy of Petroleum Fluid Monitoring Systems. *Energies* **2022**, *15*, 1986. [CrossRef]
6. Nazemi, E.; Roshani, G.H.; Feghhi, S.A.H.; Setayeshi, S.; Zadeh, E.E.; Fatehi, A. Optimization of a method for identifying the flow regime and measuring void fraction in a broad beam gamma-ray attenuation technique. *Int. J. Hydrog. Energy* **2016**, *41*, 7438–7444. [CrossRef]
7. Sattari, M.A.; Korani, N.; Hanus, R.; Roshani, G.H.; Nazemi, E. Improving the performance of gamma radiation based two phase flow meters using optimal time characteristics of the detector output signal extraction. *J. Nucl. Sci. Technol.* **2020**, *41*, 42–54.
8. Hanus, R.; Zych, M.; Petryka, L.; Świsulski, D.; Strzępowicz, A. Application of ANN and PCA to two-phase flow evaluation using radioisotopes. *EPJ Web Conf.* **2017**, *143*, 02033. [CrossRef]
9. Salgado, C.M.; Brandão, L.E.; Schirru, R.; Pereira, C.M.; da Silva, A.X.; Ramos, R. Prediction of volume fractions in three-phase flows using nuclear technique and artificial neural network. *Appl. Radiat. Isot.* **2009**, *67*, 1812–1818. [CrossRef] [PubMed]
10. Salgado, C.M.; Pereira, C.M.; Schirru, R.; Brandão, L.E. Flow regime identification and volume fraction prediction in multiphase flows by means of gamma-ray attenuation and artificial neural networks. *Prog. Nucl. Energy* **2010**, *52*, 555–562. [CrossRef]
11. Salgado, W.; Dam, R.; Salgado, C. Optimization of a flow regime identification system and prediction of volume fractions in three-phase systems using gamma-rays and artificial neural network. *Appl. Radiat. Isot.* **2021**, *169*, 109552. [CrossRef] [PubMed]
12. Sattari, M.A.; Roshani, G.H.; Hanus, R. Improving the structure of two-phase flow meter using feature extraction and GMDH neural network. *Radiat. Phys. Chem.* **2020**, *171*, 108725. [CrossRef]
13. Sattari, M.A.; Roshani, G.H.; Hanus, R.; Nazemi, E. Applicability of time-domain feature extraction methods and artificial intelligence in two-phase flow meters based on gamma-ray absorption technique. *Measurement* **2021**, *168*, 108474. [CrossRef]
14. Roshani, M.; Sattari, M.A.; Ali, P.J.M.; Roshani, G.H.; Nazemi, B.; Corniani, E.; Nazemi, E. Application of GMDH neural network technique to improve measuring precision of a simplified photon attenuation based two-phase flowmeter. *Flow Meas. Instrum.* **2020**, *75*, 101804. [CrossRef]
15. Alamoudi, M.; Sattari, M.; Balubaid, M.; Eftekhari-Zadeh, E.; Nazemi, E.; Taylan, O.; Kalmoun, E. Application of Gamma Attenuation Technique and Artificial Intelligence to Detect Scale Thickness in Pipelines in Which Two-Phase Flows with Different Flow Regimes and Void Fractions Exist. *Symmetry* **2021**, *13*, 1198. [CrossRef]
16. Roshani, M.; Phan, G.; Faraj, R.H.; Phan, N.-H.; Roshani, G.H.; Nazemi, B.; Corniani, E.; Nazemi, E. Proposing a gamma radiation based intelligent system for simultaneous analyzing and detecting type and amount of petroleum by-products. *Nucl. Eng. Technol.* **2020**, *53*, 1277–1283. [CrossRef]
17. Tkachenko, R.; Izonin, I.; Tkachenko, P. Neuro-Fuzzy Diagnostics Systems Based on SGTM Neural-Like Structure and T-Controller. In *International Scientific Conference "Intellectual Systems of Decision Making and Problem of Computational Intelligence"*; Springer: Cham, Switzerland, 2019; pp. 685–695.
18. Izonin, I.; Tkachenko, R.; Kryvinska, N.; Tkachenko, P. Multiple linear regression based on coefficients identification using non-iterative SGTM neural-like structure. In Proceedings of the International Work-Conference on Artificial Neural Networks, Gran Canaria, Spain, 12–14 June 2019; Springer: Cham, Switzerland; pp. 467–479.
19. Mayet, A.M.; Alizadeh, S.M.; Kakarash, Z.A.; Al-Qahtani, A.A.; Alanazi, A.K.; Guerrero, J.W.G.; Alhashimi, H.H.; Eftekhari-Zadeh, E. Increasing the Efficiency of a Control System for Detecting the Type and Amount of Oil Product Passing through Pipelines Based on Gamma-Ray Attenuation, Time Domain Feature Extraction, and Artificial Neural Networks. *Polymers* **2022**, *14*, 2852. [CrossRef]
20. Nussbaumer, H.J. The fast Fourier transform. In *Fast Fourier Transform and Convolution Algorithms*; Springer: Berlin, Germany, 1981; pp. 80–111.
21. Mayet, A.M.; Salama, A.S.; Alizadeh, S.M.; Nesic, S.; Guerrero, J.W.G.; Eftekhari-Zadeh, E.; Nazemi, E.; Iliyasu, A.M. Applying Data Mining and Artificial Intelligence Techniques for High Precision Measuring of the Two-Phase Flow's Characteristics Independent of the Pipe's Scale Layer. *Electronics* **2022**, *11*, 459. [CrossRef]
22. Iliyasu, A.M.; Mayet, A.M.; Hanus, R.; El-Latif, A.A.A.; Salama, A.S. Employing GMDH-Type Neural Network and Signal Frequency Feature Extraction Approaches for Detection of Scale Thickness inside Oil Pipelines. *Energies* **2022**, *15*, 4500. [CrossRef]
23. Taylor, J.G. *Neural Networks and Their Applications*; John Wiley & Sons Ltd.: Brighton, UK, 1996.

24. Gallant, A.R.; White, H. On learning the derivatives of an unknown mapping with multilayer feedforward networks. *Neural Netw.* **1992**, *5*, 129–138. [CrossRef]
25. Hosseini, S.; Roshani, G.; Setayeshi, S. Precise gamma based two-phase flow meter using frequency feature extraction and only one detector. *Flow Meas. Instrum.* **2020**, *72*, 101693. [CrossRef]
26. Peyvandi, R.G.; Rad, S.Z.I. Application of artificial neural networks for the prediction of volume fraction using spectra of gamma rays backscattered by three-phase flows. *Eur. Phys. J. Plus* **2017**, *132*, 511. [CrossRef]
27. Isaev, A.A.; Aliev, M.M.O.; Drozdov, A.N.; Gorbyleva, Y.A.; Nurgalieva, K.S. Improving the Efficiency of Curved Wells' Operation by Means of Progressive Cavity Pumps. *Energies* **2022**, *15*, 4259. [CrossRef]
28. Lalbakhsh, A.; Mohamadpour, G.; Roshani, S.; Ami, M.; Roshani, S.; Sayem, A.S.M.; Alibakhshikenari, M.; Koziel, S. Design of a Compact Planar Transmission Line for Miniaturized Rat-Race Coupler With Harmonics Suppression. *IEEE Access* **2021**, *9*, 129207–129217. [CrossRef]
29. Roshani, S.; Roshani, S. A compact coupler design using meandered line compact microstrip resonant cell (MLCMRC) and bended lines. *Wirel. Netw.* **2021**, *27*, 677–684. [CrossRef]
30. Shukla, N.K.; Mayet, A.M.; Vats, A.; Aggarwal, M.; Raja, R.K.; Verma, R.; Muqeet, M.A. High speed integrated RF–VLC data communication system: Performance constraints and capacity considerations. *Phys. Commun.* **2021**, *50*, 101492. [CrossRef]
31. Hookari, M.; Roshani, S.; Roshani, S. High-efficiency balanced power amplifier using miniaturized harmonics suppressed coupler. *Int. J. RF Microw. Comput. Aided Eng.* **2020**, *30*, e22252. [CrossRef]
32. Mayet, A.M.; Hussain, A.M.; Hussain, M.M. Three-terminal nanoelectromechanical switch based on tungsten nitride, an amorphous metallic material. *Nanotechnology* **2016**, *27*, 035202. [CrossRef]
33. Lotfi, S.; Roshani, S.; Roshani, S.; Gilan, M.S. Wilkinson power divider with band-pass filtering response and harmonics suppression using open and short stubs. *Frequenz* **2020**, *74*, 169–176. [CrossRef]
34. Mayet, A.; Hussain, M. Amorphous WNx Metal for Accelerometers and Gyroscope. In Proceedings of the MRS Fall Meeting, Boston, MA, USA, 30 November–5 December 2014.
35. Jamshidi, M.; Siahkamari, H.; Roshani, S.; Roshani, S. A compact Gysel power divider design using U-shaped and T-shaped resonators with harmonics suppression. *Electromagnetics* **2019**, *39*, 491–504. [CrossRef]
36. Mayet, A.; Smith, C.E.; Hussain, M.M. Energy reversible switching from amorphous metal based nanoelectromechanical switch. In Proceedings of the 2013 13th IEEE International Conference on Nanotechnology (IEEE-NANO 2013), Beijing, China, 5–8 August 2013; pp. 366–369.
37. Roshani, S.; Roshani, S. Two-section impedance transformer design and modeling for power amplifier applications. *Appl. Comput. Electromagn. Soc. J. (ACES)* **2017**, *32*, 1042–1047.
38. Jamshidi, M.B.; Roshani, S.; Talla, J.; Roshani, S.; Peroutka, Z. Size reduction and performance improvement of a microstrip Wilkinson power divider using a hybrid design technique. *Sci. Rep.* **2021**, *11*, 7773. [CrossRef] [PubMed]
39. Mayet, A.; Smith, C.; Hussain, M.M.; Smith, C. Amorphous metal based nanoelectromechanical switch. In Proceedings of the 2013 Saudi International Electronics, Communications and Photonics Conference, Riyadh, Saudi Arabia, 27–30 April 2013; pp. 1–5. [CrossRef]
40. Hookari, M.; Roshani, S.; Roshani, S. Design of a low pass filter using rhombus-shaped resonators with an analytical LC equivalent circuit. *Turk. J. Electr. Eng. Comput. Sci.* **2020**, *28*, 865–874. [CrossRef]
41. Pirasteh, A.; Roshani, S.; Roshani, S. Design of a miniaturized class F power amplifier using capacitor loaded transmission lines. *Frequenz* **2020**, *74*, 145–152. [CrossRef]
42. Roshani, S.; Dehghani, K.; Roshani, S. A lowpass filter design using curved and fountain shaped resonators. *Frequenz* **2019**, *73*, 267–272. [CrossRef]
43. Roshani, S.; Roshani, S. Design of a compact LPF and a miniaturized Wilkinson power divider using aperiodic stubs with harmonic suppression for wireless applications. *Wirel. Netw.* **2020**, *26*, 1493–1501. [CrossRef]
44. Alanazi, A.K.; Alizadeh, S.M.; Nurgalieva, K.S.; Guerrero, J.W.G.; Abo-Dief, H.M.; Eftekhari-Zadeh, E.; Nazemi, E.; Narozhnyy, I.M. Optimization of X-ray Tube Voltage to Improve the Precision of Two Phase Flow Meters Used in Petroleum Industry. *Sustainability* **2021**, *13*, 13622. [CrossRef]
45. Alanazi, A.K.; Alizadeh, S.M.; Nurgalieva, K.S.; Nesic, S.; Guerrero, J.W.G.; Abo-Dief, H.M.; Eftekhari-Zadeh, E.; Nazemi, E.; Narozhnyy, I.M. Application of Neural Network and Time-Domain Feature Extraction Techniques for Determining Volumetric Percentages and the Type of Two Phase Flow Regimes Independent of Scale Layer Thickness. *Appl. Sci.* **2022**, *12*, 1336. [CrossRef]
46. Mohamadinia, A.; Shama, F.; Sattari, M.A. Miniaturized bandpass filter using coupled lines for wireless applications. *Frequenz* **2021**, *75*, 301–308. [CrossRef]
47. Jedkare, E.; Shama, F.; Sattari, M.A. Compact Wilkinson power divider with multi-harmonics suppression. *AEU Int. J. Electron. Commun.* **2020**, *127*, 153436. [CrossRef]
48. Tabatabaee, A.H.; Shama, F.; Sattari, M.A.; Veysifard, S. A miniaturized Wilkinson power divider with 12th harmonics suppression. *J. Electromagn. Waves Appl.* **2020**, *35*, 371–388. [CrossRef]